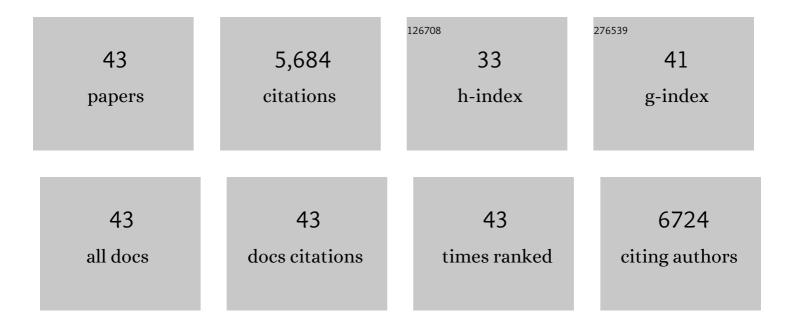
Santosh Kumar

List of Publications by Year in descending order

Source: https://exaly.com/author-pdf/3043086/publications.pdf Version: 2024-02-01



#	Article	IF	CITATIONS
1	Synthesis of a novel and stable g-C3N4–Ag3PO4 hybrid nanocomposite photocatalyst and study of the photocatalytic activity under visible light irradiation. Journal of Materials Chemistry A, 2013, 1, 5333.	5.2	584
2	Fe-doped and -mediated graphitic carbon nitride nanosheets for enhanced photocatalytic performance under natural sunlight. Journal of Materials Chemistry A, 2014, 2, 6772.	5.2	536
3	Phase Transformation Synthesis of Novel Ag ₂ O/Ag ₂ CO ₃ Heterostructures with High Visible Light Efficiency in Photocatalytic Degradation of Pollutants. Advanced Materials, 2014, 26, 892-898.	11.1	443
4	g-C ₃ N ₄ /NiAl-LDH 2D/2D Hybrid Heterojunction for High-Performance Photocatalytic Reduction of CO ₂ into Renewable Fuels. ACS Applied Materials & Interfaces, 2018, 10, 2667-2678.	4.0	438
5	Cost-effective and eco-friendly synthesis of novel and stable N-doped ZnO/g-C3N4 core–shell nanoplates with excellent visible-light responsive photocatalysis. Nanoscale, 2014, 6, 4830.	2.8	433
6	Synthesis of Magnetically Separable and Recyclable g-C ₃ N ₄ –Fe ₃ O ₄ Hybrid Nanocomposites with Enhanced Photocatalytic Performance under Visible-Light Irradiation. Journal of Physical Chemistry C, 2013, 117, 26135-26143.	1.5	358
7	Cobalt promoted TiO2/GO for the photocatalytic degradation of oxytetracycline and Congo Red. Applied Catalysis B: Environmental, 2017, 201, 159-168.	10.8	298
8	Construction of Bi2WO6/RGO/g-C3N4 2D/2D/2D hybrid Z-scheme heterojunctions with large interfacial contact area for efficient charge separation and high-performance photoreduction of CO2 and H2O into solar fuels. Applied Catalysis B: Environmental, 2018, 239, 586-598.	10.8	278
9	P25@CoAl layered double hydroxide heterojunction nanocomposites for CO 2 photocatalytic reduction. Applied Catalysis B: Environmental, 2017, 209, 394-404.	10.8	200
10	Direct Z-Scheme g-C ₃ N ₄ /FeWO ₄ Nanocomposite for Enhanced and Selective Photocatalytic CO ₂ Reduction under Visible Light. ACS Applied Materials & Interfaces, 2019, 11, 6174-6183.	4.0	197
11	g-C3N4-Based Nanomaterials for Visible Light-Driven Photocatalysis. Catalysts, 2018, 8, 74.	1.6	188
12	Facile synthesis of hierarchical Cu2O nanocubes as visible light photocatalysts. Applied Catalysis B: Environmental, 2016, 189, 226-232.	10.8	132
13	Graphite-protected CsPbBr3 perovskite photoanodes functionalised with water oxidation catalyst for oxygen evolution in water. Nature Communications, 2019, 10, 2097.	5.8	124
14	Cu and Fe oxides dispersed on SBA-15: A Fenton type bimetallic catalyst for N,N -diethyl- p -phenyl diamine degradation. Applied Catalysis B: Environmental, 2016, 199, 323-330.	10.8	119
15	Synthesis of novel and stable g-C ₃ N ₄ /N-doped SrTiO ₃ hybrid nanocomposites with improved photocurrent and photocatalytic activity under visible light irradiation. Dalton Transactions, 2014, 43, 16105-16114.	1.6	105
16	g-C 3 N 4 (2D)/CdS (1D)/rGO (2D) dual-interface nano-composite for excellent and stable visible light photocatalytic hydrogen generation. International Journal of Hydrogen Energy, 2017, 42, 5971-5984.	3.8	105
17	Influence of La-doping on phase transformation and photocatalytic properties of ZnTiO ₃ nanoparticles synthesized via modified sol–gel method. Physical Chemistry Chemical Physics, 2014, 16, 728-735.	1.3	93
18	Synthesis of Cr and La-codoped SrTiO ₃ nanoparticles for enhanced photocatalytic performance under sunlight irradiation. Physical Chemistry Chemical Physics, 2014, 16, 23819-23828.	1.3	88

Santosh Kumar

#	Article	IF	CITATIONS
19	N-doped C dot/CoAl-layered double hydroxide/g-C3N4 hybrid composites for efficient and selective solar-driven conversion of CO2 into CH4. Composites Part B: Engineering, 2019, 176, 107212.	5.9	86
20	Single atom Cu(I) promoted mesoporous titanias for photocatalytic Methyl Orange depollution and H2 production. Applied Catalysis B: Environmental, 2018, 232, 501-511.	10.8	75
21	All-Inorganic CsPbBr ₃ Nanocrystals: Gram-Scale Mechanochemical Synthesis and Selective Photocatalytic CO ₂ Reduction to Methane. ACS Applied Energy Materials, 2020, 3, 4509-4522.	2.5	75
22	Surface plasmon resonance-induced photocatalysis by Au nanoparticles decorated mesoporous g-C 3 N 4 nanosheets under direct sunlight irradiation. Materials Research Bulletin, 2016, 75, 51-58.	2.7	74
23	Mechanochemically synthesized Pb-free halide perovskite-based Cs ₂ AgBiBr ₆ –Cu–RGO nanocomposite for photocatalytic CO ₂ reduction. Journal of Materials Chemistry A, 2021, 9, 12179-12187.	5.2	70
24	Synthesis of highly efficient and recyclable visible-light responsive mesoporous g-C3N4 photocatalyst via facile template-free sonochemical route. RSC Advances, 2014, 4, 8132.	1.7	68
25	Polypyrrole-Promoted rGO–MoS ₂ Nanocomposites for Enhanced Photocatalytic Conversion of CO ₂ and H ₂ O to CO, CH ₄ , and H ₂ Products. ACS Applied Energy Materials, 2020, 3, 9897-9909.	2.5	61
26	Photocatalytic Activation and Reduction of CO ₂ to CH ₄ over Single Phase Nano Cu ₃ SnS ₄ : A Combined Experimental and Theoretical Study. ACS Applied Energy Materials, 2019, 2, 5677-5685.	2.5	54
27	g-C3N4/NaTaO3 organic–inorganic hybrid nanocomposite: High-performance and recyclable visible light driven photocatalyst. Materials Research Bulletin, 2014, 49, 310-318.	2.7	53
28	In situ growth strategy for highly efficient Ag2CO3/g-C3N4 hetero/nanojunctions with enhanced photocatalytic activity under sunlight irradiation. Journal of Environmental Chemical Engineering, 2015, 3, 852-861.	3.3	53
29	Sizeâ€Dependent Visible Light Photocatalytic Performance of Cu ₂ O Nanocubes. ChemCatChem, 2018, 10, 3554-3563.	1.8	44
30	Hypercrosslinked Polymers as a Photocatalytic Platform for Visibleâ€Lightâ€Driven CO ₂ Photoreduction Using H ₂ O. ChemSusChem, 2021, 14, 1720-1727.	3.6	42
31	Silver-Decorated TiO ₂ Inverse Opal Structure for Visible Light-Induced Photocatalytic Degradation of Organic Pollutants and Hydrogen Evolution. ACS Applied Materials & Interfaces, 2020, 12, 41200-41210.	4.0	41
32	Delaminated CoAlâ€Layered Double Hydroxide@TiO ₂ Heterojunction Nanocomposites for Photocatalytic Reduction of CO ₂ . Particle and Particle Systems Characterization, 2018, 35, 1700317.	1.2	40
33	In situ phase transformation synthesis of unique Janus Ag 2 O/Ag 2 CO 3 heterojunction photocatalyst with improved photocatalytic properties. Applied Surface Science, 2018, 445, 555-562.	3.1	37
34	PrFeO ₃ Photocathodes Prepared Through Spray Pyrolysis. ChemElectroChem, 2020, 7, 1365-1372.	1.7	27
35	Template-free and eco-friendly synthesis of hierarchical Ag3PO4 microcrystals with sharp corners and edges for enhanced photocatalytic activity under visible light. Materials Letters, 2014, 123, 172-175.	1.3	22
36	Strategies for the deposition of LaFeO ₃ photocathodes: improving the photocurrent with a polymer template. Sustainable Energy and Fuels, 2020, 4, 884-894.	2.5	15

Santosh Kumar

#	Article	IF	CITATIONS
37	Two-dimensional materials for photocatalytic water splitting and CO2 reduction. , 2020, , 173-227.		7
38	Dielectric behaviour of sodium and potassium doped magnesium titanate. Bulletin of Materials Science, 2012, 35, 1165-1171.	0.8	6
39	Hierarchical ZnO "rod like―architecture synthesized via reverse micellar route for improved photocatalytic activity. Materials Letters, 2013, 101, 33-36.	1.3	6
40	Enhancement of photocatalytic efficiency using heterostructured SiO2–Ta2O5 thin films. Materials Research Express, 2015, 2, 056404.	0.8	5
41	Nanocatalysts for CO2 Conversion. RSC Catalysis Series, 2019, , 207-235.	0.1	2
42	Recent Advances in Photocatalytic Materials for Solar Fuel Production from Water and Carbon Dioxide. RSC Energy and Environment Series, 2020, , 80-115.	0.2	2
43	Solar energy harvesting with carbon nitrides. , 2022, , 81-107.		0